Development of a Control Strategy to Maximize System Performance for Heat Pump Systems

Jiazhen Ling, Ph.D., Research Associate, Yunho Hwang Ph.D., Research Professor, Vikrant Aute Ph.D., Assistant Research Scientist, Reinhard Radermacher Ph.D., Professor,
4164 Glenn Martin Hall Building, Center for Environmental Energy Engineering, University of Maryland, College Park, MD, 20742, USA
Kyle Gluesenkamp, Ph.D., RND Staff, Oak Ridge National Laboratory, Oak Ridge, TN, USA

Abstract: In this paper, a new control strategy is proposed and applied to an adsorption heat pump system as an example. A 2 kW cooling capacity adsorption heat pump using zeolite was constructed and powered by waste heat from a 4 kW internal combustion engine. Over 145 test points were obtained under various ambient conditions, chilled water temperatures, adsorption time and heat recovery time. To extend the range of data to a complete design space, those test points were used to develop a model using a sophisticated interpolation technique called the Kriging method. The Kriging model predicted the system COP, capacity, etc., based on a full factorial expansion of the four inputs. With the help of the model, multiple-coefficient curve fit functions were created to simulate COP, adsorption time and heat recovery time depending on the evaporating, condensing temperatures and cooling capacity. Those functions served as the control strategy to determine the optimal adsorption and heat recovery time associated with maximum COP. The developed control strategy was evaluated by the test facility and demonstrated a good accuracy of ±10% as compared with experimental data.

Key Words: heat pumps, adsorption, control strategy, optimization

1 INTRODUCTION

The performance of heat pump systems is typically evaluated by two metrics, heating/cooling capacity and coefficient of performance (COP), and one can often find them from the product specifications. These two values are often obtained by experimental measurements under some standard test conditions such as those defined in the ASHRAE standard 116 (ASHRAE 2010). Therefore, it is common for manufacturers to tune their products to have an optimal performance under such standard rating conditions. However, heat pump systems are subject to operate under a wide range of ambient conditions and are operated in longer hours other than rating conditions. For most heat pump products that cannot afford to have built-in sophisticated control units, it is impossible for them to provide optimum performance in every ambient conditions as they do at the rated condition. Take adsorption heat pump cycles as an example. What is the optimal adsorption/desorption time under different ambient conditions? We may generalize all these questions to the following question. Can we come up with a control strategy that depending on different ambient (external) conditions, the system can find an optimal way of operation by changing some internal parameters?

In this paper, a novel approach for developing a control strategy, which is capable of determining the optimal system operating parameters of an adsorption system depending on various ambient conditions and load requirements, is presented. Although it is exemplified by the adsorption heat pump system, the approach itself is a general one so that it can be applicable to other heat pump cycles or even those systems for application beyond the HVAC field. Since many readers may not be familiar to the adsorption cycle, some background information on its operation is provided first and the development of the control strategy is described.

2 BACKGROUND

2.1 Operation of adsorption system

A traditional adsorption heat pump system consists of an adsorber, a desorber, an evaporator, a condenser and valves, as illustrated in Figure 1. The adsorber and desorber are heat exchangers (HXs) coated with adsorbent material such as zeolite and are placed in separate sealed vessels (chambers). The two chambers are filled with refrigerant, i.e., water vapor, and have internal piping allowing heat transfer fluid (HTF) to either heat or cool the refrigerant. As the HTF heats the refrigerant, the refrigerant is desorbed from the surface of absorbent bed and becomes refrigerant vapor. As more refrigerant vapor is desorbed from the surface of the adsorption bed, the internal pressure of the chamber increases. Once the pressure exceeds that of the upper condenser, the vapor flows towards the condenser due to the pressure difference. In the condenser, the refrigerant vapor is condensed by rejecting heat to HTF at ambient temperature. In the meantime, the HTF becomes warmer and can be used to provide heating. The resulting refrigerant liquid passes through an expansion valve with part of which flashes and becomes low pressure two-phase fluid. It then evaporates in the evaporator and provides cooling to the chilled water. After the evaporation, the refrigerant becomes vapor and is sent to the other chamber called adsorber. The low pressure vapor is then adsorbed by the adsorbent material coated on the surface of heat exchanger. The above process continues until all the refrigerant is desorbed from the desorber and the adsorber is saturated with refrigerant. The role of the two chambers can now be switched and they repeat the above process with the refrigerant flowing in a reversed direction.

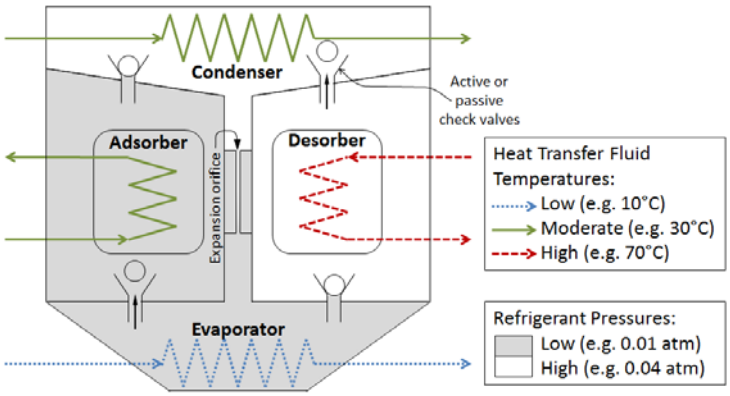


Figure 1: Illustration of a simple adsorption heat pump

2.2 Control parameters for adsorption systems

Traditional adsorption heat pumps have a relatively low COP when it is compared with that of the vapor compression cycle. Therefore, researchers have been proposing different approaches in order to improve its efficiency. As one of those methods, heat recovery (HR) process can be implemented in adsorption chillers.

In order to explain the benefits of adding the HR process, one should first have a close look at the batch operating mode of adsorption cycles. As was pointed out in the last section, the two chambers operate alternatively while functioning as adsorber and desorber. When a chamber works as an adsorber, the HTF circulating within is typically at ambient temperature such as 30°C. It serves as a heat sink for refrigerant vapor to be adsorbed. As the adsorption continues, the chamber eventually becomes saturated. It then has to work as a desorber. At this time, hot water at around 70°C starts circulating inside the chamber in order to provide energy for the refrigerant to be desorbed from adsorbent material. Ideally, all the energy from hot water should be used to desorb refrigerant, however, this does not end up being realistic. Part of the

energy from hot water has to be spent on increasing the wall temperature of heat exchanger, and when considering the thermal mass of the heat exchanger, such amount of energy required is not a small fraction. Now consider the other chamber that is currently used as either a desorber or a to-be adsorber. It requires cooling to reduce the wall temperature from around 70°C to 30°C. Therefore, an immediate solution is to connect these two chambers so that the HTF can flow from one to the other. Such connection makes the HTF in the desorber to preheat the thermal mass of adsorber while the HTF in the adsorber to precool that of desorber. Generally, the HR improves COP because it reduces the amount of energy wasted in heating and cooling heat exchanger thermal mass. However, since the process of HR does not produce heating/cooling, it may actually reduce the capacity of the entire system by extending the cycle time. Figure 2 demonstrates the COP and capacity as a function of HR time. It is clear that for different ambient conditions, there exists an optimal HR time.

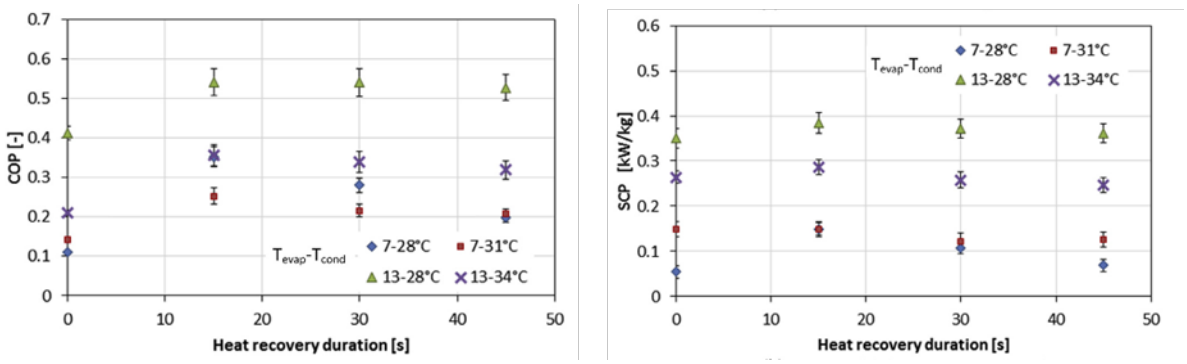


Figure 2: System COP and capacity as a function of heat recovery time (Qian et al., 2013)

Another parameter that affects the cycle performance is the time of adsorption/desorption. Generally speaking, the longer that time, more refrigerant can be adsorbed onto/desorbed from the surface of the heat exchanger, and therefore, for a fixed amount of energy inputs, it has more outputs. Nevertheless, since the adsorption/desorption performance is hardly a linear process against time, a too long adsorption/desorption time may in fact reduce the system capacity when the quotient of energy generated by extended time divided the extended time is small. Figure 3 explains that the control of adsorption time may generate optimal COP and capacity.

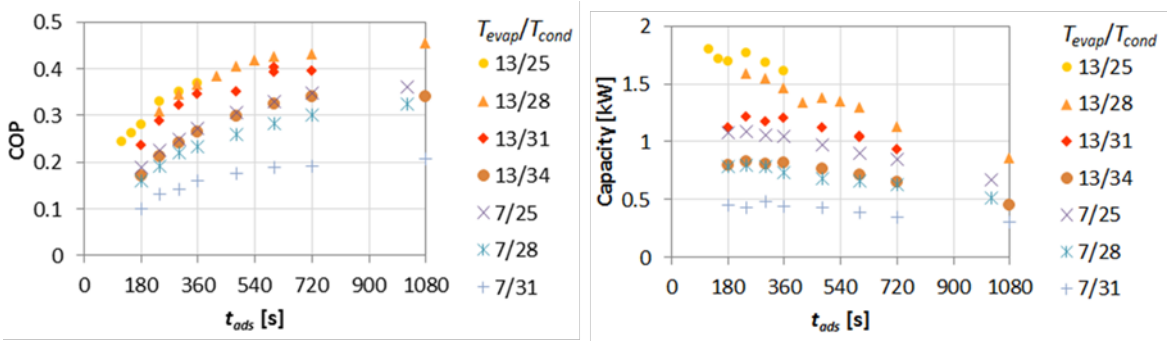


Figure 3: System COP and capacity as a function of adsorption time (Gluesenkamp, 2012)

2.3 Experimental setup

In order to experimentally evaluate the performance of the adsorption heat pump, a test facility was built. A photograph of the experiment set up is shown in Figure 4, where the four vacuum chambers can be seen, each with a clear plastic front cover. The condenser is in the top-most chamber, and the evaporator in the lowest. The other two chambers house the adsorber heat exchangers. The chambers were connected by 5 cm diameter electronically actuated ball

valves and insulated 5 cm diameter copper tube. Later, insulation was added to the adsorber chambers, the flanges and front of the condenser and evaporator (not shown in Figure 4). Additional basic specifications of the adsorption chiller are listed in Table 1. Since heat recovery process is difficult to be discerned in the facility, a schematic diagram of the system is demonstrated in Figure 5 where the green lines represent the heat recovery loop.

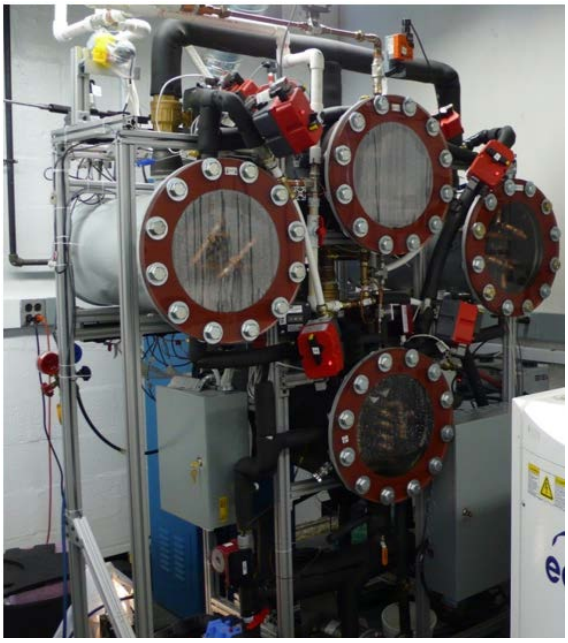


Figure 4: Picture of the adsorption system

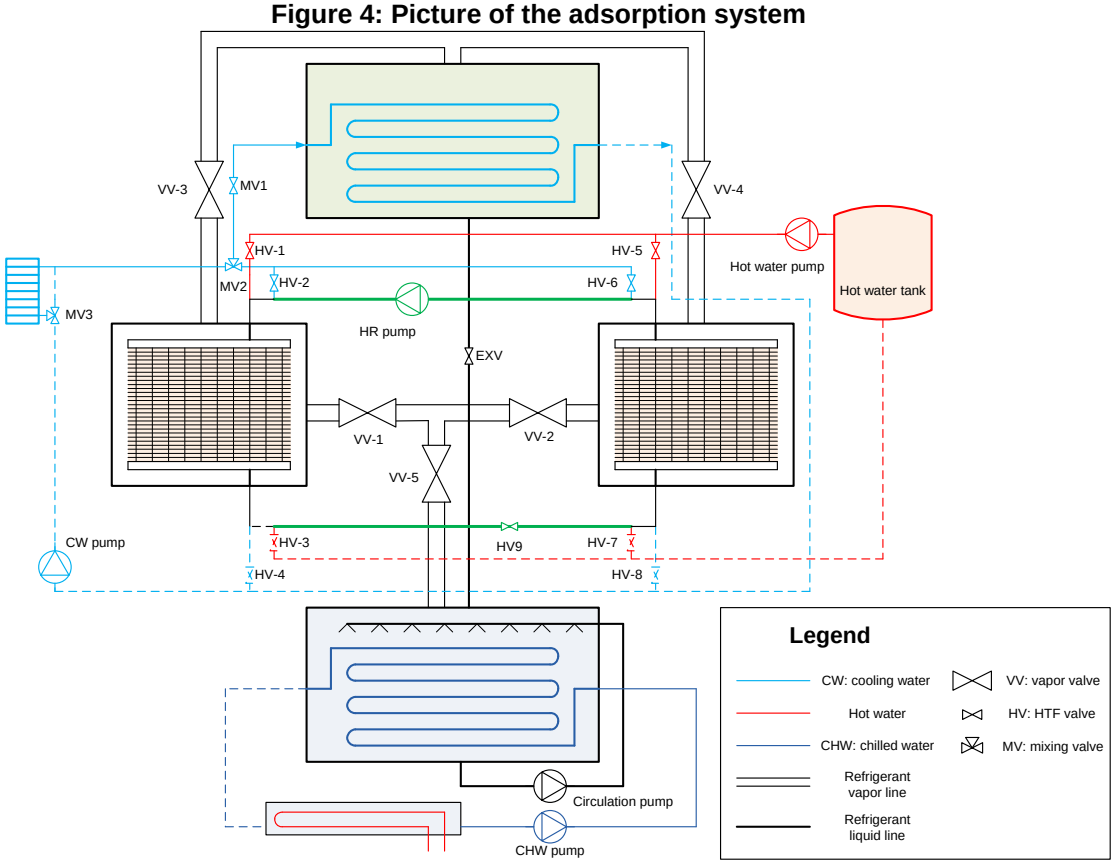


Figure 5: Schematic of the adsorption system with heat recovery (Qian et al., 2013)

Table 1: Specifications of adsorption chiller

Nominal cooling capacity	2 kW
Number of adsorber HXs	2
Working pair (refrigerant/adsorbent)	water/zeolite
Adsorber HX finned-volume dimensions (excludes headers and u-tubes)	600 x 264 x 102 mm
Calculated adsorbent mass (per HX)	2.82 kg
Adsorbent substrate area (per HX)	16.7 m^2
Charge of HTF (per HX, excl. headers)	2.47 liter

3 DEVELOPMENT OF CONTROL STRATEGY

3.1 Extend experimental data using Kriging models

The experimental heat pump results were used to develop a control strategy for the heat pump. In this section, the authors discuss the development of control strategy using Kriging method. The reasons we chose Kriging method over other traditional response surface method for constructing approximations are accuracy and relatively lower computational cost. Based on Simpson et al. (2001), Kriging method provides slightly better accuracy for four different optimization problems in terms of numerical error analysis and graphical analysis. In those examples, Kriging models use only one constant term for the global portion of the model in conjunction with a Gaussian correlation function, and therefore has relatively little added computational cost.

As it being discussed in the previous sections, two time constants (time of heat recovery and time of adsorption/desorption) affect the system performance so that they should be optimized based on different operating conditions. The purpose of the control strategy is to select a pair of system operating parameters (cycle time t_{ads} and heat recovery time t_{HR}) that provides a maximum efficiency given ambient conditions (T_{cond} and T_{evap}) and desired capacity ($Q_{desired}$). The control strategy establishes a relationship between internal and external conditions as a function of capacity. A schematic of the control strategy is depicted in Figure 6. In the figure, Q_{cf} represents the actual capacity can be supplied by the adsorption system.

Figure 7 shows the flow chart of the proposed approach that obtain curve fits for t_{ads} and t_{HR} based on experimental results. As mentioned before, the proposed method can be applied to other systems, a generalized nomenclature is used hereby:

- N = number of discretizations in each state variable
- $\underset{\sim}{x}$ = internal state variables
- $\underset{\sim}{y}$ = external state variables
- $\underset{\sim}{z}$ = performance (or response) variables
- c = capacity
- p = # of variables in $\underset{\sim}{x}$
- q = # of variables in $\underset{\sim}{y}$

As is this work, the following values are used:

- N = 10
- $\underset{\sim}{x}$ = t_{ads}, t_{HR}
- $\underset{\sim}{y}$ = T_{cond}, T_{evap}
- $\underset{\sim}{z}$ = COP, Q
- p = 2
- q = 2

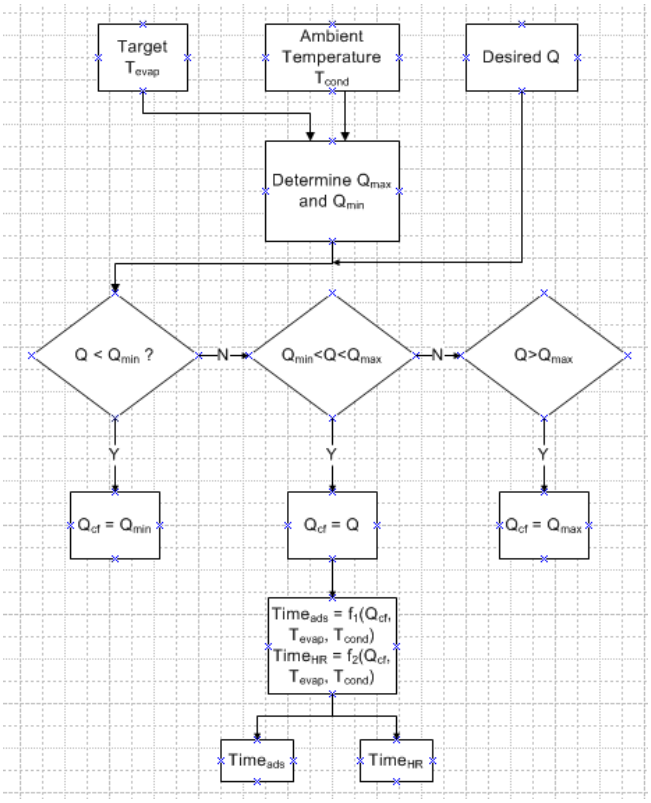


Figure 6: Schematic of control strategy evaluation

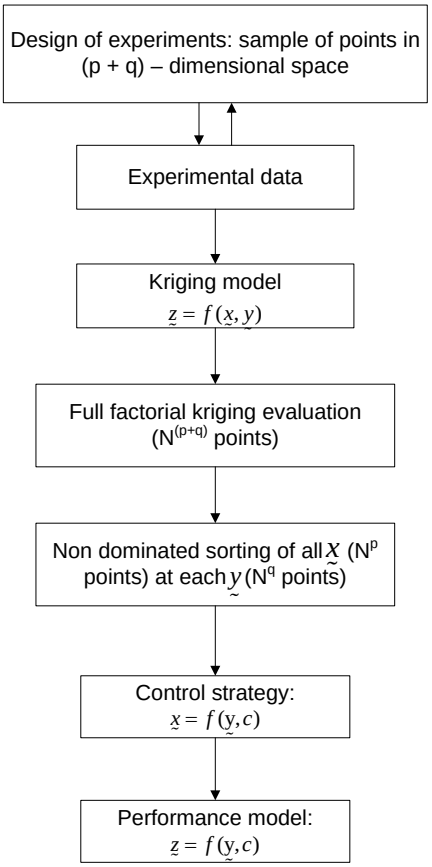


Figure 7: Overview of control strategy and empirical model development (Gluesenkamp, 2012)

A Kriging model was first developed using 145 steady state experimental data from the aforementioned test facility. A Kriging model (Simpson et al., 2001) is created by using a sophisticated interpolation method that curve fits the outputs (responses) based on inputs (variables). In this case, there are four variables: condenser temperature, evaporator temperature, adsorption time and heat recovery time. The first two variables are external operating parameters that represent ambient conditions, and the latter two are internal operating parameters meaning they are adjustable parameters in the system. Since the Kriging method generates curve fit functions, it can evaluate a single set of inputs, meaning one operating conditions under one ambient condition, within a second. The fast calculation speed makes it a critical intermediate step which allows for a full factorial evaluation over a sample of 100 internal variables (10 t_{ads} values by 10 t_{HR} values) and a sample of 100 external conditions (10 condenser by 10 evaporator temperatures) for a total of 10,000 Kriging evaluations. This full factorial evaluation in turn allowed non-dominated sorting to establish a well-populated Pareto front at each external state.

Next, the Krging model was validated by using the so called the leave-one-out (LOO) method. The method, for every 145 experimental data points, 144 points were used to develop the Kriging model and the one left was used to validate the model. The error in the prediction for this point is denoted ε_{LOO}. A value of ε_{LOO} can be calculated for each of 145 points by repeating the construction of 145 separate Kriging models, resulting in 145 values of ε_{LOO}. Figure 8 shows the predicted values using the LOO method versus all 145 experimental values of COP. To have a practical meaning, those points with COP <=0.1 are filtered. The overall comparison demonstrates the Kriging models predict most COP values within ±10% errors.

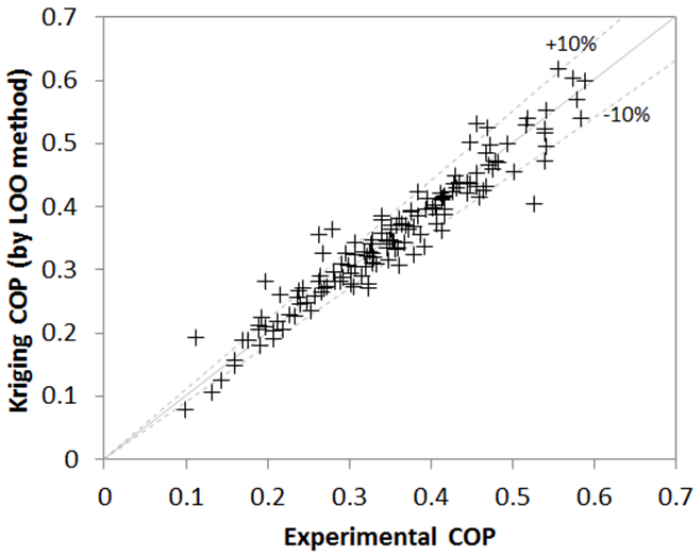


Figure 8: Kriging predictions vs. 145 experimental points using LOO method

With the help of the validated Kriging models, it is now possible to extend our 145 test data to 10,000 full factorial points. For a clear illustration, Figure 9 demonstrates only a sample of 2,500 points (100 internal states over 25 external conditions). The results are plotted in a response-space plot (COP vs. capacity). It is the goal that the heat pump should always operate at the maximum COP and therefore, the red points in the figure, also called Pareto points, are the desired ones. Since there are 25 external points meaning 25 different ambient conditions, there exists 25 sets of Pareto solutions that guarantee for each capacity there is one corresponding pair of internal parameters that achieves highest COP. Note that, for clarity, not all points are shown: a filter has been applied based on thresholds of COP>0.1 and Capacity>0.1 kW (as a result there are only 22 Pareto sets shown in Figure 9).

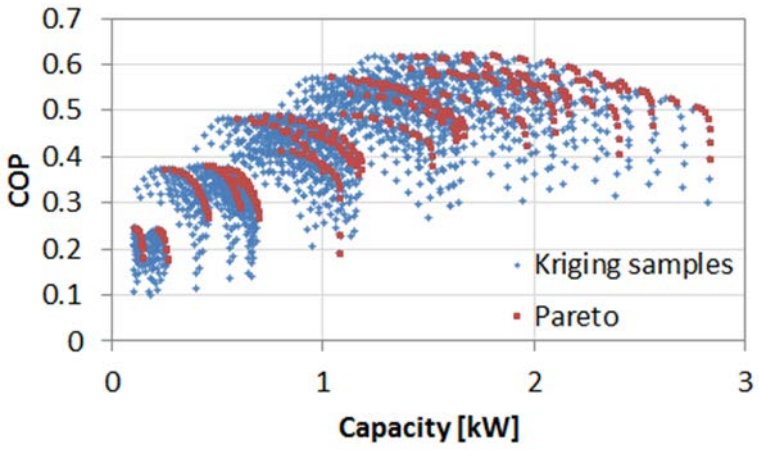


Figure 9: Pareto sets in response-space for operation at 25 external conditions

Out of the 10,000 points sampled by Kriging model evaluation, 1,525 met threshold criteria and were non-dominated (i.e. Pareto). These were distributed among 86 of the 100 external conditions – 14 external conditions had no internal conditions capable of meeting the threshold requirements of COP>0.1 and Capacity>0.1 kW. Figure 10 shows the 86 external conditions, in terms of evaporating and condensing temperatures, having performance meeting the threshold criteria. It can be seen that a limit on temperature lift of about 25°C was observed in experimental tests. This is clear from the figure since an imaginary line along the border between feasible and infeasible has a slope of about 1, and $T_{cond} - T_{evap} \approx 25$°C along that imaginary line.

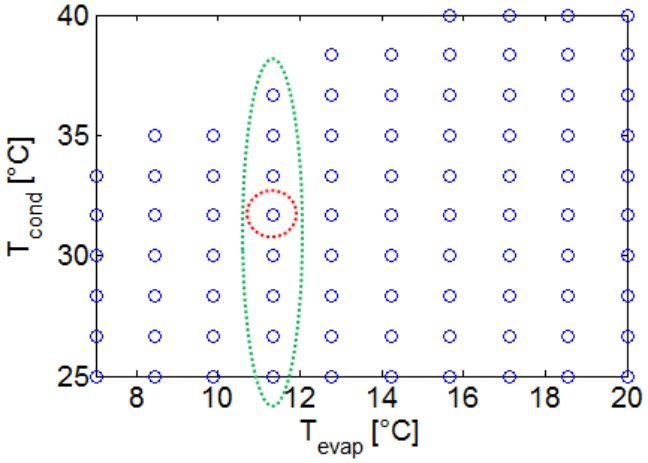


Figure 10: External conditions with COP>0.1 and capacity>0.1 kW

To further illustrate the method, Pareto points at 11.3°C evaporating temperature, circled in green in Figure 10, are expanded in response-space in Figure 11 to show their performance. When seen in performance-space, it is clear that capacity is consistently dropping off as heat rejection temperature rises, until the heat pump is no longer able to meet the capacity threshold above 37°C condensing temperature.

Next, the single external condition circled in red in Figure 10 and Figure 11 is expanded to show the effects of internal cycle variables on performance at a single external condition. This is shown in Figure 12. Note that only 18 of the original 100 combinations of internal operating variables turned out to be Pareto points. These 18 Pareto points make up Figure 12, are all shown in the red circled region in Figure 11, and collapse to a single (red-circled) point in Figure 10.

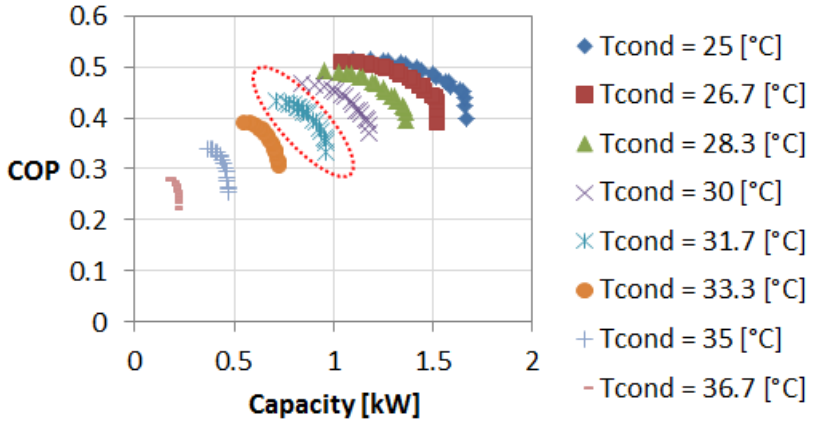


Figure 11: Solutions circled in green from previous figure in performance-space

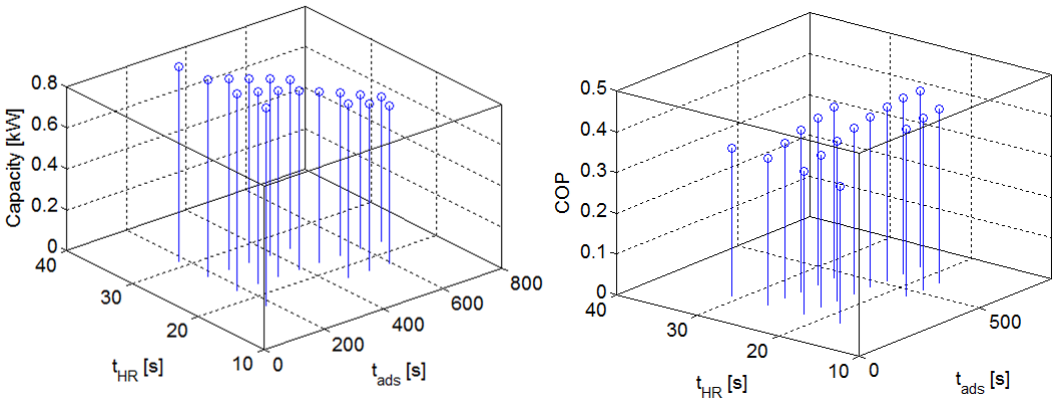


Figure 12: Performance as a function of cycle times for condition circled in red in previous two figures

By examination of Figure 12, the tradeoff between COP and capacity with respect to adsorption time can be seen: within the range of about 180 to 660 seconds, longer adsorption times result in higher COP but lower capacity. Adsorption times below or above this range are not present in the Pareto set: both COP and capacity suffer outside this Pareto range.

The same general trends also hold for heat recovery times, although the effect is not discernible from visual inspection of Figure 12. A heat recovery duration less than 15 seconds always resulted in a dominated solution for this set of external conditions. This is not true for every external condition, however, since at some external conditions t_{HR}=0 is included in the Pareto set.

3.2 Curve fitted model for Pareto sets

In order to better apply the control strategy to practice, several 6-coefficient or 10-coefficient second order polynomial curve fit models are formed to describe those Pareto sets. Each of the following was curve fitted:

- COP = $f(T_{evap}, T_{cond}, Q_{desired})$
- $Q_{min} = f(T_{evap}, T_{cond})$
- $Q_{max} = f(T_{evap}, T_{cond})$
- $t_{ads} = f(T_{evap}, T_{cond}, Q_{desired})$
- $t_{HR} = f(T_{evap}, T_{cond}, Q_{desired})$

Each curve fit was verified by comparison with the Kriging prediction across the set of 1,525 Pareto samples. An example result, for COP, is shown in Figure 13.

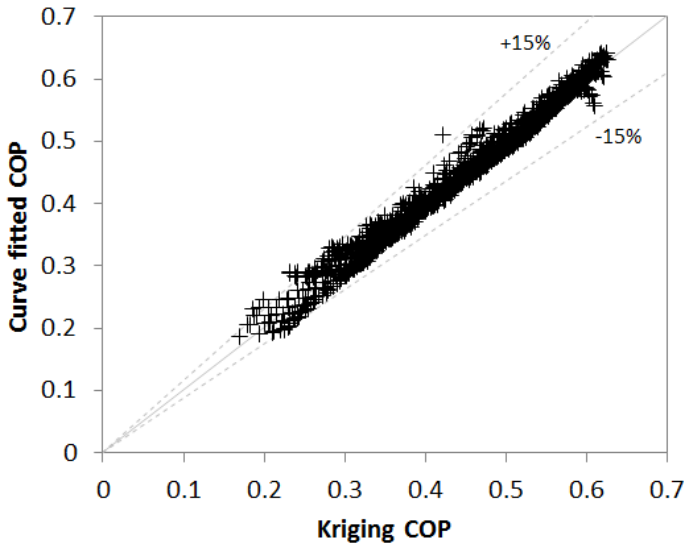


Figure 13: Comparison of curve fitted and Kriging-predicted COP for Pareto points

The 6-coefficient curve fits for Q_{min} and Q_{max} are second-order polynomial functions of two variables, T_{evap} and T_{cond}. They can be evaluated using Eq. 1 and Table 2. The 10-coefficient curve fits for COP, t_{ads} and t_{HR} are also second-order polynomials, but are functions of three variables (T_{cond}, T_{evap}, and Q_{evap}). They can be evaluated using Eq. 2 and Table 3.

$$Q_{min}, Q_{max} = \sum_{i=1}^{6} k_i T_{evap}^{m_i} T_{cond}^{n_i} \quad (1)$$

Table 2: Coefficients for curve fits for Q_{min} and Q_{max}

i	k_i (Q_{min})	k_i (Q_{max})	m_i	n_i
1	-6.385E-04	3.829E-04	2	0
2	1.986E-03	1.567E-03	1	1
3	4.181E-02	8.703E-02	1	0
4	-3.900E-03	-4.211E-03	0	2
5	1.351E-01	1.183E-01	0	1
6	-7.593E-01	-1.503E-01	0	0

$$COP, t_{ads}, t_{HR} = \sum_{i=1}^{10} k_i T_{evap}^{m_i} T_{cond}^{n_i} Q^{p_i} \quad (2)$$

Table 3: Coefficients for curve fits for COP, t_{ads} and t_{HR}

i	k_i (COP)	k_i (t_{ads})	k_i (t_{HR})	m_i	n_i	p_i
1	-4.899E-03	-8.733E+00	-2.233E-01	2	0	0
2	8.621E-03	1.585E+01	3.054E-01	1	1	0
3	5.122E-02	8.389E+01	3.524E+00	1	0	1
4	-1.385E-01	-2.074E+02	-7.345E+00	1	0	0
5	-4.996E-03	-1.035E+01	-7.731E-02	0	2	0
6	-4.202E-02	-5.869E+01	-2.669E+00	0	1	1
7	1.994E-01	3.715E+02	3.845E+00	0	1	0
8	-1.655E-01	1.986E+00	-1.874E+01	0	0	2
9	7.471E-01	-5.460E+02	8.290E+01	0	0	1
10	-1.675E+00	-1.958E+03	-3.857E+01	0	0	0

Together, the curve fits for COP, Q_{min} and Q_{max} form an empirical model that can be used for heat pump simulations and performance prediction as shown in Figure 6. The curve fits for Q_{min}, Q_{max}, t_{ads} and t_{HR} can be used to develop a control strategy for heat pump operation.

3.3 Validations of the control strategy

The established control strategy is then validated by experiments. A total twenty points are randomly selected and the COP is first predicted by using the above 10 coefficient models. Those twenty points have minimum evaporating and condensing temperatures of 7°C and 27°C, respectively. The maximum evaporating and condensing temperatures are 20°C and 43°C, respectively. These two ranges cover almost the entire practical operating conditions of adsorption heat pumps. The adsorption/desorption time varies between 240 seconds to 720 seconds while the heat recovery time span between 15 seconds to 30 seconds. Experiments were then conducted under each ambient conditions with specified time constants. The resulting experimental COP were plotted against the curve fitted predictions. Seventeen out of twenty points falls within a ±10% deviation region (Figure 14). It proves that the developed model predicts the system COP reasonably well. Therefore, it can be used for system control.

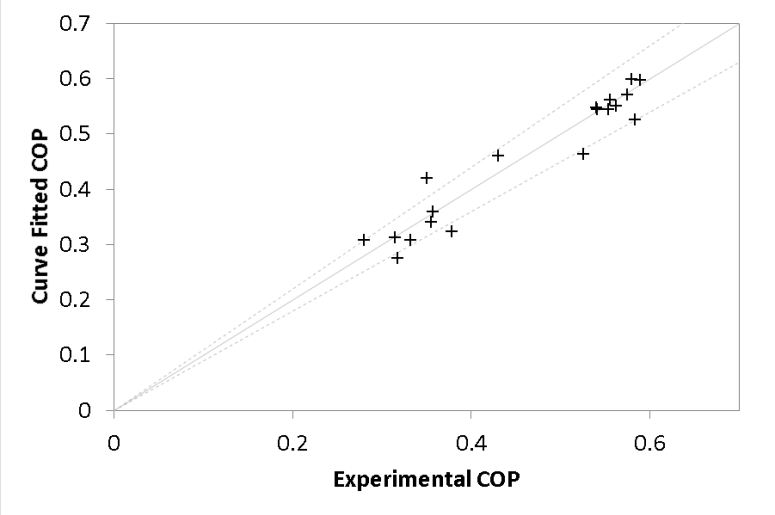


Figure 14: Proposed control strategy validation

4 CONCLUSIONS

The authors proposed a novel approach to develop a control strategy that determines the optimal operating parameters based on various ambient conditions. The approach starts with developing Kriging models using a limited 145 test data. With the help of Kriging models, it is capable of predicting the adsorption cycle performance for 10,000 different combinations of ambient conditions (in terms of evaporating and condensing temperatures) and operating conditions (in terms of adsorption/desorption time and heat recovery time). By plotting the results onto a capacity-COP plot, one can easily observe the maximum possible COP at various ambient conditions and capacities. Based on the Kriging model outputs, polynomial equations for capacity and COP as functions of ambient conditions are generated. As the final step, the COP predicted by those polynomial equations were compared against experimental data. Seventeen out of a total twenty points fall within ±10% error region. It proves the success of the developed control strategy.

5 NOMENCLATURES

Abbreviations

COP coefficient of performance

HVAC heating, ventilation and air conditioning
HR heat recovery *or* heat recuperation
HTF heat transfer fluid
HX heat exchanger
LOO leave-one-out method
Q heat transfer [kW]
Q_{cf} Real capacity can be achieved by the system [kW]
q heat flux [W/m^2]
T temperature [K or ^{O}C]

Greek Symbols
ε error

Subscripts
ads adsorbent
cond condenser
des desorption
evap evaporator
HR heat recovery (for prime mover or adsorption chiller)
ref refrigerant *or* reference

6 ACKNOWLEDGEMENT

The support of this research through the Center for Environmental Energy Engineering at the University of Maryland is gratefully acknowledged.

7 REFERENCES

ASHRAE/ANSI, Methods of Testing for Rating Seasonal Efficiency of Unitary Air Conditioners and Heat Pumps, ANSI/ASHRAE standard 116-2010, American Society of Heating, Refrigerating and Air-conditioning Engineers, Inc. Atlanta.

Suxin Qian, Kyle Gluesenkamp, Yunho Hwang, Reinhard Radermacher, Ho-Hwan Chun, Cyclic steady state performance of adsorption chiller with low regeneration temperature zeolite, Energy, Volume 60, 1 October 2013, Pages 517-526, ISSN 0360-5442, http://dx.doi.org/10.1016/j.energy.2013.08.041.

Kyle Gluesenkamp, 2012, DEVELOPMENT AND ANALYSIS OF MICRO POLYGENERATION SYSTEMS AND ADSORPTION CHILLERS, Ph.D Dissertation, University of Maryland, College Park.

T.W. Simpson, T.M. Mauery, J.J.Korte, F. Mistre, 2001, Kringing Models for Global Approximation in Simulation-Based Multidisciplinary Design Optimization, AIAA Journal, Vol. 39, No. 12, pp. 2233 – 2241.